Available online at www.sciencedirect.com
SCIENCE DIRECT®
International Journal of Refractory Metals & Hard Materials 23 (2005) 233–241
International Journal of REFRACTORY METALS & HARD MATERIALS
www.elsevier.com/locate/ijrmhm

Liquid phase sintering of functionally graded WC–Co composites

O. Eso [a], Z. Fang [a,*], A. Griffo [b]

[a] Department of Metallurgical Engineering, University of Utah, 135 South 1460 East Room 412, Salt Lake City, Utah 84112, USA
[b] Smith International, Inc., Houston, Texas, USA

Received 11 November 2004; accepted 12 April 2005

Abstract

Functionally graded cemented tungsten carbide (WC–Co) is an example of functionally graded materials (FGM) in which mechanical properties are optimized by the presence of microstructural gradients such as cobalt gradient and grain size differences within the microstructure. In particular, a cobalt gradient is preferred. However, the manufacture of FGM WC–Co with a cobalt gradient is difficult because the flow of the liquid phase during liquid phase sintering (LPS) would eliminate any initial cobalt gradient built into the powder compacts. In this paper, different factors, which can be used to influence the migration of liquid during sintering, are investigated. These factors include gradients in grain size, carbon and cobalt content, and sintering time. It is shown that a difference in particle size may induce a step-wise profile of cobalt concentration. Initial carbon content differences, however, can be used to obtain a gradient of cobalt during sintering. The effects of these factors are explained based on the roles of capillary force and phase reactions.

Keywords: Cemented tungsten carbide; Functionally graded WC–Co; Liquid phase sintering; Cobalt gradient; Capillary force

1. Introduction

A functionally graded hard material is a composite material that has a microstructural gradient [1]. Functionally graded hard materials offer advantages in terms of the fracture toughness and wear resistance combinations in comparison to conventional homogeneous WC–Co materials [2,3]. Functionally graded WC–Co composites are a unique example of functionally graded hard materials. Typically, a functionally graded WC–Co exhibits a gradient in WC grain size and/or cobalt composition resulting in a property gradient across the microstructure.

Typical cemented carbide manufacturing processes rely on liquid phase sintering for densification. Attempts have been made to produce functionally graded WC–Co composites using liquid phase sintering. However, during liquid phase sintering, the liquid can easily flow and any initial gradient of cobalt content, that might have been built into a powder compact, is eliminated [4,5]. This makes the processing of functionally graded WC–Co difficult. A solution to this problem is to use pressure assisted sintering at solid state. However, liquid phase sintering is the most viable and economical method for producing functionally graded WC–Co if the cobalt gradient can be maintained or created during liquid phase sintering.

There are two existing industrial technologies that produce functionally graded cemented tungsten carbides. One example is cutting tools made of cemented tungsten carbides with cobalt-enriched surfaces. This class of cutting tools has tougher edges because the cobalt content in the surface layer is higher than that in the bulk [6]. Different methods have been used to produce cemented tungsten carbides with cobalt-enriched surfaces [6–8]. Most of these methods rely on controlling

* Corresponding author. Tel.: +1 801 581 8128; fax: +1 801 581 4937.
E-mail address: zfang@mines.utah.edu (Z. Fang).

0263-4368/$ - see front matter © 2005 Elsevier Ltd. All rights reserved.
doi:10.1016/j.ijrmhm.2005.04.017

nitrogen potentials during sintering. However, it is also known that carbon content is a factor that affects the formation of the cobalt enriched surface layer.

Another example is the so-called Dual Properties carbide. Dual properties carbides are produced using a process based on diffusion during a separate heat treatment [9]. During the heat treatment, pre-sintered parts that are carbon deficient are subjected to a carbon rich atmosphere and the diffusion of carbon into the part results in a cobalt gradient. However, there is presently no published theoretical work on the principles and mechanism of formation of Dual Properties carbide.

Both the cobalt enriched WC–Co and the dual properties carbide processes indicate that carbon is a factor, which can be used to alter or influence the distribution of cobalt in a WC–Co sample. Fang and Eso recently studied the effect of carbon gradient on the development of cobalt gradient during liquid phase sintering using a bi-layer WC–Co sample with an initial difference in carbon content between the two layers [10]. The initial difference in carbon content was created by pressing two powders with different carbon contents together. It was found that, when there is an initial difference in carbon contents, cobalt appears to migrate in the direction of carbon diffusion during sintering resulting in a gradient of cobalt in the sample. It has also been reported that a difference in grain size within a WC–Co sample could also induce a gradient in cobalt during sintering [11].

Evidently, there are multiple factors that affect the cobalt distribution in WC–Co materials during liquid phase sintering. However, there is a lack of detailed studies of the effects of these factors, the interactions between them, or the underlying principles. In order to develop methodologies for the manufacture of functionally graded WC–Co, this study investigates the effects of various factors including carbon and cobalt content, grain sizes, and sintering time on the formation of the graded microstructure. The underlying principles governing the cobalt phase migration and distribution are examined based on the roles of capillary force and phase reactions during sintering with the aim of gaining a comprehensive understanding of the phenomena.

2. Experimental

WC–Co powders with different cobalt contents (6%, 10%, and 16% by weight) and particle sizes (1 μm and 5 μm) were used for this study. All the raw materials of graded WC–Co powders had stoichiometric carbon content. Hereafter, the term ''total carbon content'' will refer to the WC–Co composite, to distinguish it from carbon content of WC only. In order to create a carbon gradient in a powder prior to sintering, tungsten powders were added to WC–Co powders to reduce the total carbon content below the stoichiometric value while pure graphite powders were added to the WC–Co powders to increase the total carbon content above the stoichiometric value in the alloy. The powder mixtures were ball milled using a rolling mill for 16 h in heptane. After milling, the powders were dried in a rotavapor under vacuum. The dried WC–Co powders were cold pressed at 200 MPa. in a rigid die into laminate disks (19.4 mm dia. × 4 mm thick) consisting of two layers. Each layer has a different predetermined composition.

Table 1 shows the composition of samples with different particle sizes but identical cobalt and carbon content in the two layers. Table 2 shows the composition of samples with different cobalt contents but identical particle size and carbon content in the two layers. Table 3 shows the composition of samples with different total carbon content in the two layers but identical particle size and cobalt contents. Table 4 shows the composition of samples with different cobalt and total carbon contents in the two layers but identical particle size.

Table 1
Composition of bi-layers WC–Co with an initial difference in particle size

Layers	Composition	Total carbon content
Layer 1	WC–10%Co (1 μm)	Stoichiometric
Layer 2	WC–10%Co (5 μm)	Stoichiometric

Table 2
Composition of bi-layers WC–Co with an initial difference in cobalt content

Layers	Composition	Total carbon content
Layer 1	WC–6%Co	Stoichiometric
Layer 2	WC–16%Co	Stoichiometric

Table 3
Composition of bi-layers WC–Co with an initial difference in carbon content

Layers	Composition	Total carbon content (wt%)
Layer 1	WC–10%Co	6.0
Layer 2	WC–10%Co	5.0

Table 4
Composition of bi-layer WC–Co with an initial difference in cobalt and carbon contents

Layers	Composition	Total carbon content (wt%)
Layer 1	WC–6%Co	6.1
Layer 2	WC–16%Co	4.7

The samples were sintered in a vacuum furnace at 1400 °C for 60 min. The sintered bi-layer samples were ground and polished to 1 μm finish for microstructural examinations. The cobalt distribution in the WC–Co bi-layers was measured using the Energy Dispersive Spectroscopy (EDS) on the SEM. Each data point on the cobalt distribution profile was generated by averaging EDS scans over an area of 0.2 mm by 12 mm.

3. Results

3.1. Effects of initial particle size differences

Fig. 1 shows the SEM micrograph of a bi-layer WC–Co specimen listed in Table 1 and sintered at 1400 °C. The bi-layer specimen had a nominal cobalt content of 10% by weight in both layers. Each layer had WC grain size of 1 μm and 5 μm respectively. Fig. 2 shows the cobalt distribution profile of the bi-layer WC–Co specimen in Fig. 1 measured using EDS. A stepwise profile of cobalt concentration is observed between the two layers after sintering due to the difference of particle sizes. The cobalt content in the layer with 5 μm WC grain size decreased to approximately 8% by weight while the layer with 1 μm WC grain size increased to approximately 12% by weight.

3.2. Effects of initial differences in cobalt contents

Fig. 3 shows a micrograph of WC–Co bi-layer from Table 2 sintered at 1400 °C. The total carbon content in both layers is stoichiometric. The initial cobalt content in one layer was 6% by weight while the other layer had 16% by weight. After liquid phase sintering, as expected, the cobalt content has completely homogenized across the two layers after sintering at 1400 °C for 1 h. The homogenized cobalt content of the sintered part is approximately 12% by weight.

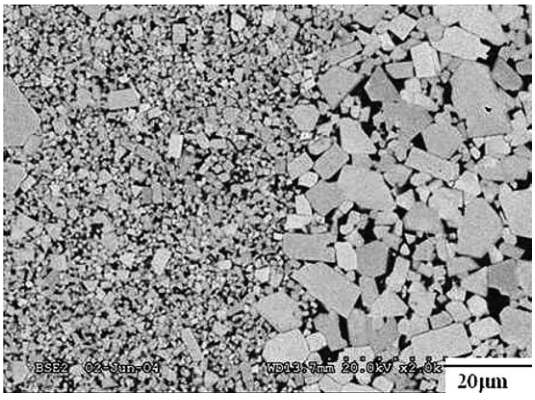

Fig. 1. SEM micrograph of WC—10%Co bi-layer with difference in grain size sintered at 1400 °C for 1 h.

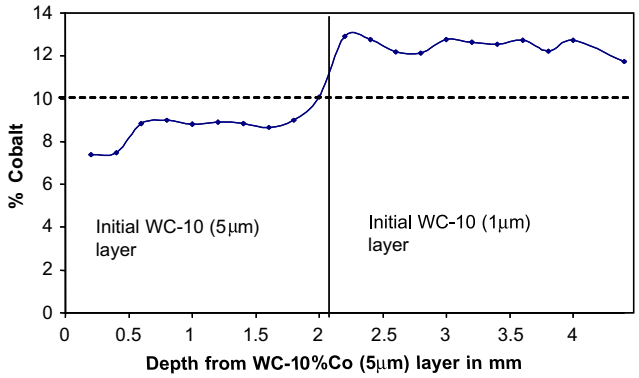

Fig. 2. Distribution of cobalt in a WC—10%Co bi-layer specimen with difference in grain size sintered at 1400 °C for 1 h.

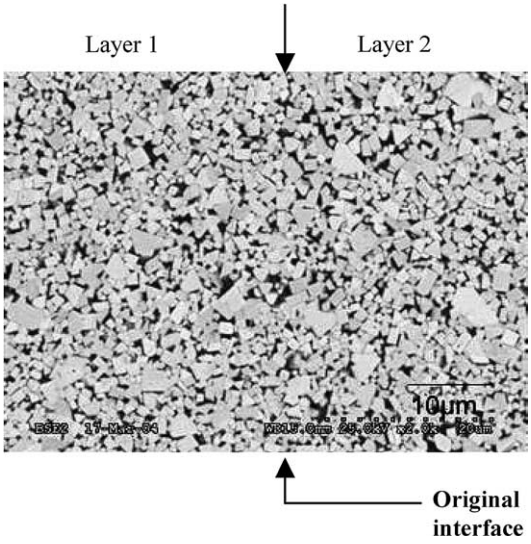

Fig. 3. SEM micrograph of WC–Co bi-layer with identical grain sizes and stoichiometric carbon content but different initial cobalt contents in the layers sintered at 1400 °C for 1 h.

3.3. Effect of initial differences in carbon contents

Fig. 4 shows the cobalt distribution in a bi-layer WC–Co specimen from Table 3 sintered at 1400 °C. Both layers had an initial cobalt content of 10% by weight. The total carbon content in one layer was reduced significantly below the stoichiometric value to 5.0% by weight while the total carbon content in the other layer was increased above the stoichiometric value to 6.0% by weight such that η phase and free carbon will form in the layers respectively at the sintering temperature if they are sintered separately. It can be seen from Fig. 4 that a gradient of cobalt is created after sintering the two layers together as a bi-layer specimen. The cobalt content varied gradually from 8% in the layer initially with excess total carbon content to about 13% in the layer initially with a

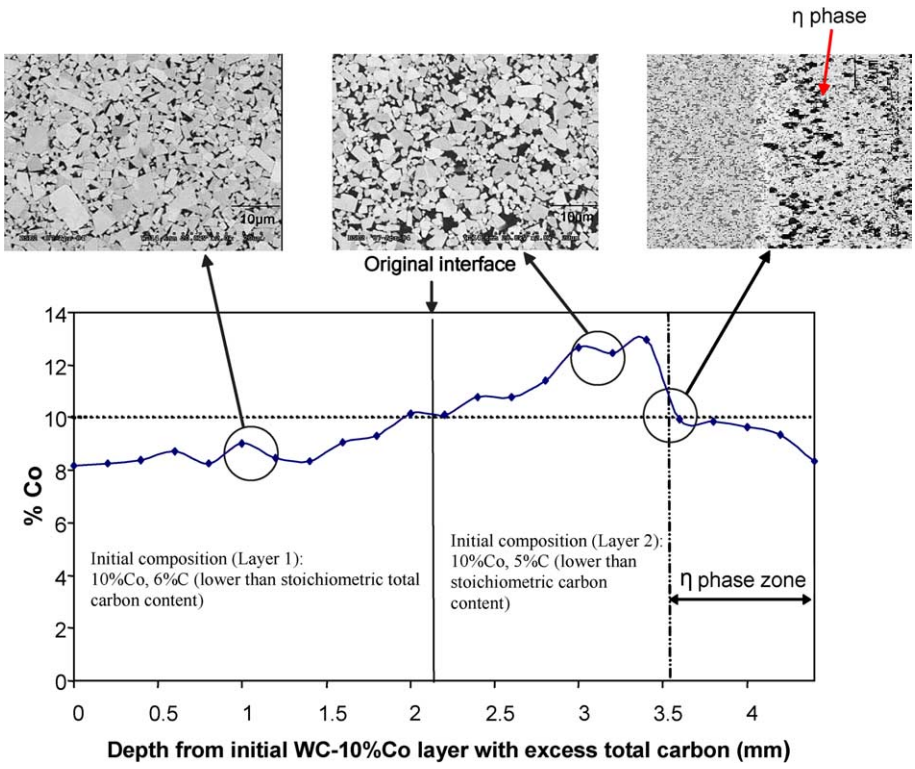

Fig. 4. Cobalt distribution in a WC–Co bi-layer specimen with identical initial cobalt content and grain sizes but different initial total carbon content sintered at 1400 °C for 1 h.

deficiency in total carbon content. The micrographs in Fig. 4 shows the different microstructure zones formed in the sample after sintering. A η phase zone can be observed towards the edge of the layer which was carbon deficient. This shows that there was only partial homogenization of carbon across the structure. In this η phase zone, there is a sudden decrease in cobalt content below the nominal value and just outside the η phase zone the highest cobalt peak of about 13% is observed.

3.4. Effects of initial differences in both carbon and cobalt contents

Fig. 5 shows micrographs of WC–Co specimen from Table 4. In the green state, the total carbon content in the layer with relatively low cobalt content (6%) was increased to 6.1% by weight, which is significantly higher than the stoichiometric total carbon content. The total carbon content in the other layer with relatively high cobalt content (16%) was reduced to 4.7%, which is significantly lower than the stoichiometric total carbon content. Fig. 5(a) and (b) shows the microstructures of each layer sintered separately. The WC—6%Co layer with high carbon content shows free carbon while the WC—16%Co layer, with low carbon content, shows η phase in their microstructures respectively. Fig. 5(c) shows the microstructure of the bi-layer specimen (two layers pressed together) after liquid phase sintering. It shows no free-carbon nor η phase in the microstructure. This indicates that the excess carbon has reacted with the η phase. The carbon content has completely homogenized across the bi-layers and the final part has stoichiometric total carbon content. The cobalt content, however, was not homogenized across the two layers. Fig. 6 shows the EDS analysis of the cobalt concentration profile of the bi-layer WC–Co samples with identical particle sizes and an initial difference in cobalt and carbon contents. In the same figure, the cobalt concentration profile of bi-layer WC–Co specimen with identical particle sizes, an initial difference in cobalt contents and stoichiometric carbon contents in the layers is shown for the purpose of comparison. It is evident that the bi-layer WC–Co sample with an initial difference in carbon content shows a cobalt gradient after sintering at 1400 °C. However, there is no cobalt gradient in the bi-layer sample initially with stoichiometric carbon content after sintering at 1400 °C. It appears from the above results that cobalt migrates in the direction of carbon diffusion.

3.5. Effects of sintering time

Fig. 7 demonstrates the kinetics of the cobalt gradient formation process. As the sintering time is increased, the

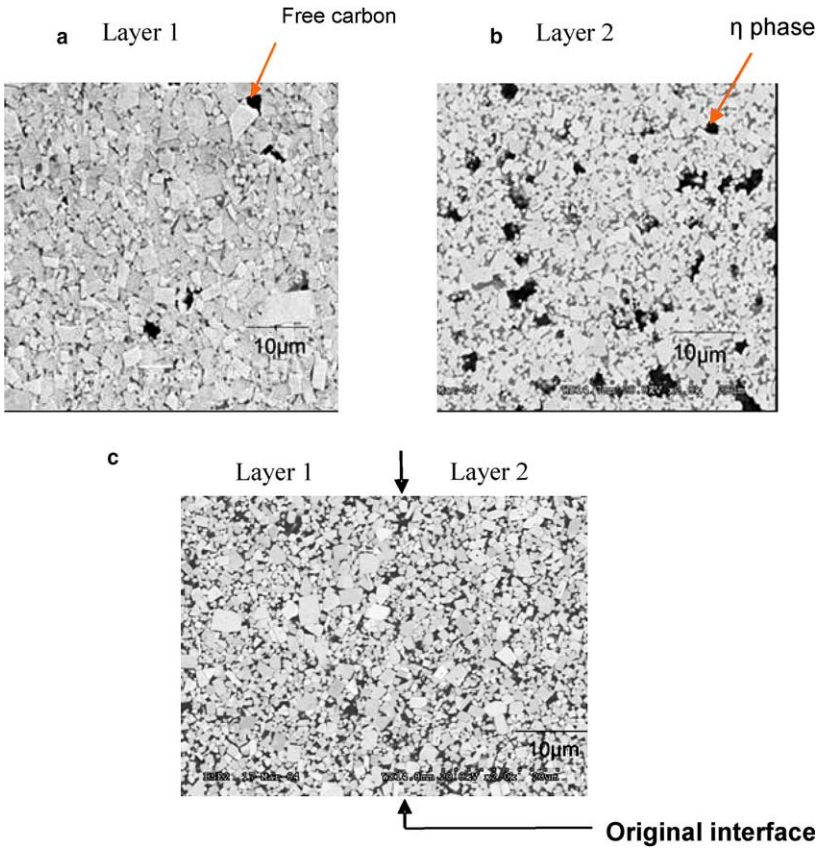

Fig. 5. SEM Micrographs of (a) WC–Co with high total carbon content (b) WC–Co with low total carbon content and (c) WC–Co bi-layer with identical particle size but different initial total carbon content and cobalt content in the layers sintered at 1400 °C for 1 h.

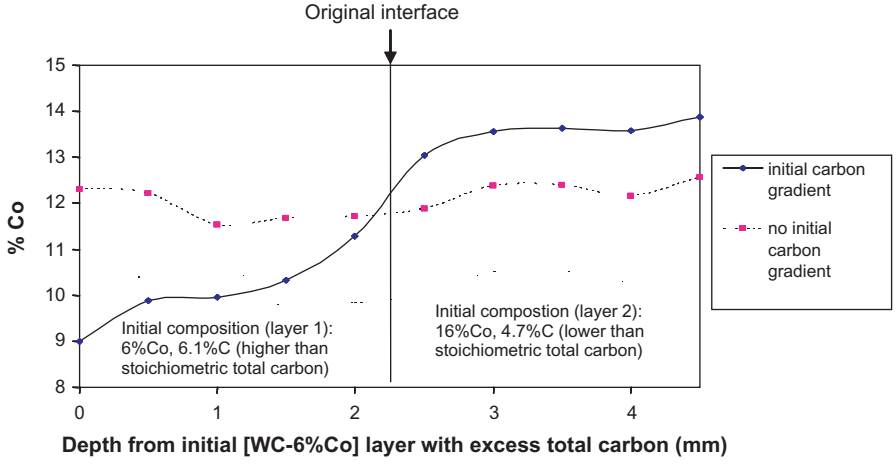

Fig. 6. Comparative plot of the cobalt distribution of WC–Co with identical initial grain sizes but different initial total carbon and cobalt contents (solid line) and WC–Co with identical grain sizes and stoichiometric carbon contents but different initial cobalt contents (dotted line) sintered at 1400 °C for 1 h.

width of the WC + Co + η zone reduces. Sintering at 1400 °C for 15 min produces WC + Co + η zone width of approximately 0.8 mm. After sintering at 1400 °C for 60 min, the width of the zone reduces to about 0.4 mm. In addition, the cobalt distribution peak and the reaction interface move in the same direction towards the edge of the sample as the sintering time is increased. This demonstrates that as the sintering time is increased, carbon diffuses further into carbon deficient layer and reacts with η phase to produce WC–Co resulting in the migration of cobalt in the same direction.

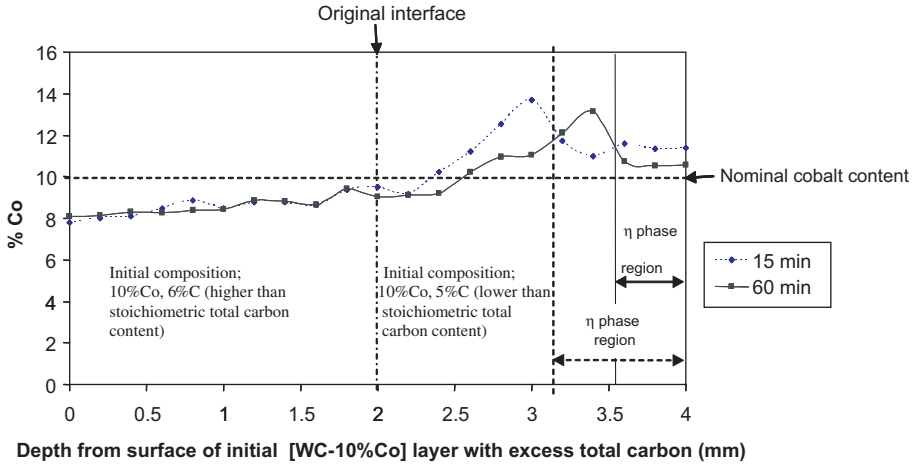

Fig. 7. Effect of sintering time on the cobalt distribution of WC–Co bi-layer with identical initial cobalt contents and grain sizes but different initial total carbon content in the layers sintered at 1400 °C.

4. Discussion

The results presented above show that functionally graded WC–Co can be manufactured by controlling critical factors such as the initial particle size, initial carbon and/or cobalt content variations, and sintering time. The final cobalt distribution in the sintered sample is the result of the combined effects of these factors on the migration of liquid phase during sintering. The migration of liquid phase can be attributed to two underlying processes. First, the basic reason for liquid flow is the difference in volume fraction of the liquid phase between graded layers during sintering. The second reason is the local chemical composition inhomogeneity, which causes local variations in the volume fraction of liquid during sintering. These two aspects are discussed as follows.

4.1. Capillary force as the driving force for cobalt migration during sintering

WC–Co, at liquid phase sintering temperature, consists of WC and liquid phase, which is primarily a cobalt solution with W and C as solutes. The liquid cobalt is uniformly distributed in between WC grains throughout the structure. The size of the cobalt pools is measured by mean free path (MFP) between WC grains. MFP is a function of cobalt content as well as grain size. When two WC–Co layers with different cobalt content are placed adjacent to each other, the flow of liquid between the two layers will be determined by the difference in capillary force between them. This problem can be modeled as an array of interconnected liquid channels between the tungsten carbide particles. The average size of these channels can be approximated by the MFP.

In the case of bi-layers with initial cobalt content differences but identical particle size and carbon content as shown in Fig. 4, at the liquid phase sintering temperature, the layer with higher cobalt content will have wider liquid channels in comparison with the layer with lower cobalt content. The structure of these liquid channels is illustrated in Fig. 8a. If the average sizes of the channels (MFP) in layers with higher and lower cobalt content are d_1 and d_2 respectively then d_1 is greater than d_2. The liquid channels present in the two layers are analogous to a system of interconnected capillaries. Based on the principles of capillarity, a narrow capillary sucks out wetting liquid from a wider capillary due to the difference in capillary force [12]. Thus, liquid will flow from the layer, initially with higher cobalt content, into the

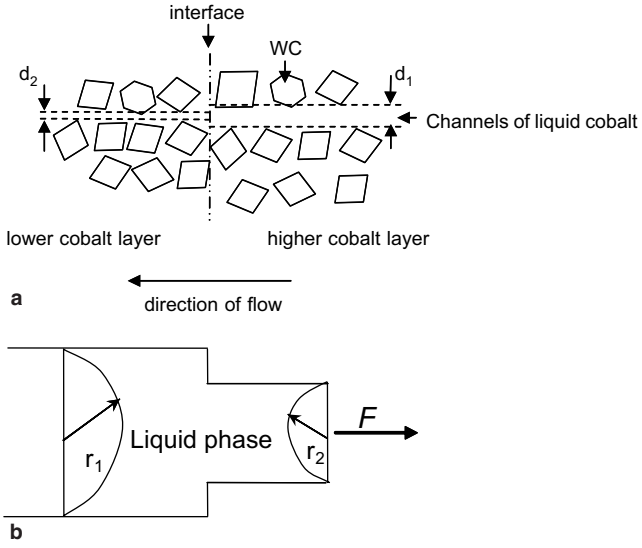

Fig. 8. An illustrative diagram of (a) liquid channels formed during sintering of WC–Co bi-layer with identical grain size but different initial cobalt contents in the layers. (b) Cylindrical capillary tube with two different cross sections.

layer initially with lower cobalt content through the interconnected liquid channels by capillary force. This will cause the layer initially with lower cobalt content to swell due to the increase in liquid content and the layer initially with higher cobalt content will shrink due to the decrease in liquid content although the total liquid content in the sample is conserved. As the liquid phase flows, d_1 will decrease while d_2 will increase since the wetting liquid will not flow out of the sample. The flow of liquid ceases when $d_1 = d_2$ and the difference in capillary force is zero.

A difference in WC grain size will also produce a difference in the size of liquid channels formed during sintering. Finer grains form smaller liquid channels while coarser grains form larger liquid channels. Thus, liquid cobalt will flow into the layer with finer WC grain size by capillary force during sintering. This capillary force is expressed in equation [1] and illustrated in Fig. 8.

$$F = 2\pi\sigma\left(\frac{r_1^2}{r_2} - \frac{r_2^2}{r_1}\right) \quad (1)$$

where F is the difference in capillary force (N) acting on the small and large menisci in Fig. 8b, σ is the surface tension (N/m), r_1 and r_2 are the radii of curvature of the large and small menisci respectively.

4.2. The effect of carbon on the volume fraction of liquid formed during sintering

During liquid phase sintering at 1400 °C, which is significantly higher than the eutectic temperature, equilibrium phase composition consists of WC and liquid cobalt phase. The volume fraction of the liquid phase can vary depending on the total carbon content in the alloy [13]. Significant deviations below or above the stoichiometric carbon content will result in the occurrence of three phase equilibrium structure involving WC + Co + W_3Co_3C (η) or WC + Co + C (graphite) respectively. The formation of W_3Co_3C (η) phase in WC–Co during sintering ties up part of the cobalt phase, which leads to the reduction of the volume fraction of the liquid phase at the sintering temperature. The dependence of volume fraction of liquid on the carbon content can be modeled based on thermodynamic equilibrium calculations. Fig. 9 shows the volume fraction of liquid phase as a function of the carbon content of WC–Co alloy used for this study [14]. The plots were generated using thermodynamic software (Thermo-Calc). The thermodynamic database for cemented carbides is available in literature [15]. Evidently, from these plots, any local inhomogeneity in carbon content within a WC–Co system will result in a corresponding difference in volume fraction of liquid, which could lead to cobalt migration.

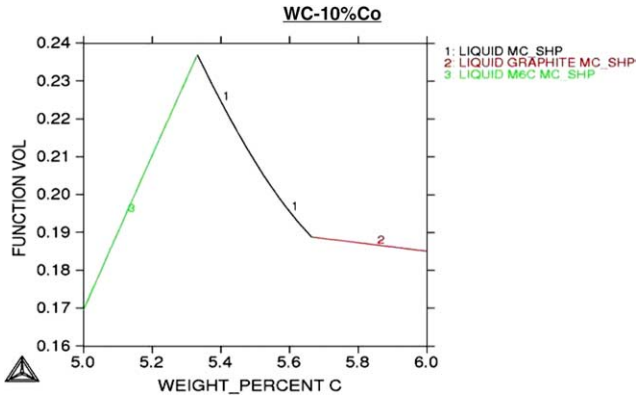

Fig. 9. Calculated volume fraction of liquid as a function of total carbon content of WC—10%Co at 1400 °C.

4.3. A qualitative model of the formation of cobalt gradient

Based on the experimental results of this study and the two underlying factors discussed above, there are three categories of possible scenarios which could result in the formation of cobalt gradient during sintering.

4.3.1. When there is no initial carbon content difference, but there are initial cobalt and/or particle size differences

When there is identical initial carbon content but a difference in initial cobalt content and/or particle size in the two graded WC–Co layers, cobalt migration is driven by capillary force only. When there is only a difference in particle size in the two layers as shown in Fig. 1, cobalt will migrate from the layer with coarser grain size to the layer with finer grain size due to capillary force. A difference in particle size will produce a stepwise profile of cobalt concentration. However, when the initial particle size is the same, but there is an initial difference in cobalt content between the two layers as shown in Fig. 4, cobalt will migrate from the layer with a higher cobalt content to the layer with a lower cobalt content due to the difference in capillary force.

4.3.2. When there is an initial carbon content difference, but there are no initial cobalt and/or grain size differences

In the case where the initial cobalt and particle size are identical but the initial carbon contents of the two layers are different as shown in Fig. 4, the cobalt gradient is determined by the equilibrium phase compositions as a function of carbon concentration profile. Carbon will diffuse to create a gradient of carbon from the carbon rich layer to the carbon deficient layer due to the difference in the chemical potential of carbon between the two layers. The carbon gradient as the results of the carbon diffusion will cause the liquid phase to flow

in order to establish an equilibrium distribution of the volume fraction of the liquid phase in the sample. The shape of the distribution curve of the volume fraction of the liquid phase will be similar to the shape of the plot in Fig. 9 as a function of the carbon profile. On the other hand, the diffusing carbon will react with η phase to produce WC and liquid Co

$$2C + W_3Co_3C \Rightarrow 3WC + 3Co \quad (L) \qquad (2)$$

This reaction releases cobalt, which contributes to the volume fraction of the liquid phase near the reaction front.

This process is schematically illustrated in Fig. 10. C_1 and C_2 are the initial carbon contents of the carbon-rich layer and the carbon-deficient layer respectively and C_s is the carbon content as a function of the position within the sample at time t_2. Between times t_1 and t_2, the reaction front has advanced a distance "x" within the sample. It implies that between the times t_1 and t_2, η phase in the area with length "x" in the sample has reacted with carbon and produced WC–Co as shown in Fig. 10. As carbon diffuses and the liquid phase migrates, both toward the η phase region, to establish the equilibrium profile of the volume fraction of liquid, the reaction front moves in the same direction and the cobalt distribution exhibits a similar shape during the process.

4.3.3. When there are initial carbon gradients as well as initial cobalt and/or gain size gradient

In the case when there is initial carbon content difference as well as initial cobalt and/or grain size differences, the final cobalt distribution is affected by all three factors. For example, when there is initially carbon and cobalt differences in WC–Co bi-layers as shown in Fig. 5, carbon diffusion and phase reactions counter the effect of capillary force due to the initial cobalt gradient (initial Δ%Co is10% for the example in Fig. 5). The carbon deficient layer, which forms η phase at the sintering temperature, ties up a certain fraction of the cobalt in the system. The differences in volume fractions of liquid at the sintering temperature will cause liquid to flow from the layer with a higher volume fraction of liquid to the layer with a lower volume fraction of liquid by capillary force. A difference in the chemical potential of carbon in the two layers will cause carbon to diffuse from the layer where it is in excess to the layer where it is deficient. The diffusing carbon will react with η phase, which yields WC and liquid Co. The overall shape of the distribution would be the sum of the effects of carbon diffusion and reactions with η phase and the effects of cobalt migration by capillary force as the results of difference in volume fraction of liquid due to the initial differences in cobalt and carbon contents between the two layers.

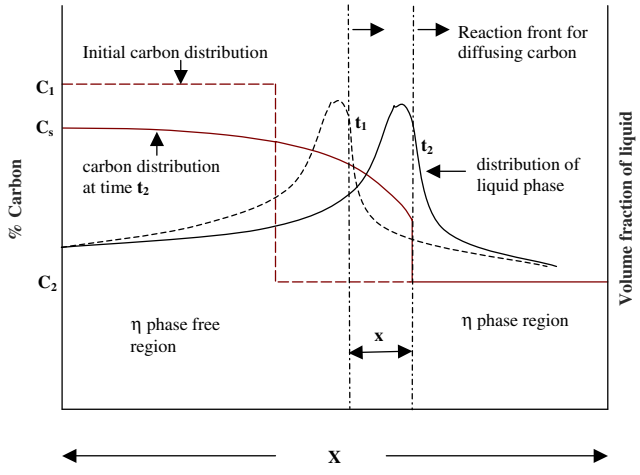

Fig. 10. Schematic diagram showing the time dependence of cobalt gradient formation during liquid phase sintering of graded WC–Co.

5. Summary

A detailed study on the effects of different factors, including grain size, carbon and cobalt contents, and sintering time, on cobalt migration during liquid phase sintering, has been performed. It was shown that initial particle size differences can induce a step-wise profile of cobalt concentration while an initial difference in carbon content can be used to obtain a cobalt gradient within the sintered WC–Co specimen. The effects of these factors are explained based on capillary force, equilibrium volume fraction of phases and phase reactions. All considered, the final cobalt distribution in the sintered functionally graded WC–Co sample is the result of the combined effects of these factors on capillary force and phase equilibrium.

Acknowledgements

The authors wish to thank Mr. Jon Bitler of Kennametal Inc. for raw materials. The financial support for one of the authors (Eso) from United States Department of Energy, Industrial Materials of the Future Program, is gratefully acknowledged.

References

[1] Tsuada K, Ikegaya A, Isobe K, Kitagawa N, Nomura T. Development of functionally graded sintered hard materials. Powder Metall 1996;39:296–300.
[2] Fang Z, Lockwood G, Griffo A. A Dual Composite of WC–Co. Metall Trans A 1999;30A:3231–8.
[3] Fang Z, Griffo A, White B, Lockwood G, Belnap D, Hilmas G, et al. Fracture resistant super hard materials and hard metals composite with functionally designed microstructure. Int J Refract Met Hard Mater 2001;19:453–9.
[4] Lisovsky AF. The migration of metals melts in sintered composite materials. Int J Heat Mass Transfer 1990;33:1599–603.

[5] Colin C, Durant L, Favrot N, Besson J, Barbier G, Delannay F. Processing of compositional gradient WC–Co cermets. In: Bildstein H, Eck R, editors. Proceedings of the 13th International Plansee seminar; 1993, 2, p. 522–36.
[6] Nemeth BJ, Grab JP, US Patent No. 4,610,931.
[7] Yohe WC. The development of cubic carbide free surface layers in cemented carbides without nitrogen. In: Bildstein H, Eck R, editors. Proceedings of the 13th International Plansee seminar; 1993, 2, p. 151–68.
[8] Yohe WC, Warren C, US Patent No. 4,548,786.
[9] Fisher, Udo KR, Hartzell, Erik T, Akerman, Jan GH, US Patent No. 4,743,515.
[10] Fang Z, Eso O. Liquid phase sintering of functionally graded WC–Co composites. Scripta Mater 2005;52:785–91.
[11] Cheng J, Wu Y, Xia Y. Fabrication of WC–Co cemented carbide with gradient distribution of WC grain size and Co composition by Tape casting. Mater Sci Forum 2003;423–425: 45–8.
[12] Luikov AV. Heat and mass transfer in capillary porous bodies. 1st English ed. London: Pergamon; 1966.
[13] Urhenius B. Evaluation of molar volumes in Co–WC system and calculation of volume fraction of phases in cemented carbides. Int J Refract Met Hard Mater 1993–94;12:121–7.
[14] Wang H, Yu Y. Private Communications, 2004.
[15] Frisk K, Dumitrescu L, Ekroth M, Jansson B, Kruse O, Sundman B. Development of a database for cemented carbides: thermodynamic modeling and experiments. J Phase Equilibria 2001; 22:645–55.